Optical time-of-flight measurement of carrier transport in $GaAs/Al_xGa_{1-x}As$ and $In_{0.53}Ga_{0.47}As/In_{0.52}Al_{0.48}As$ multiquantum wells

S. Gupta, L. Davis, and P. K. Bhattacharya
Solid State Electronics Laboratory and Ultrafast Science Laboratory, Department of Electrical Engineering and Computer Science, University of Michigan, Ann Arbor, Michigan 48109-2122

(Received 19 September 1991; accepted for publication 6 January 1992)

An all-optical time-of-flight technique is used for measuring perpendicular carrier transport in semiconductor heterostructures and multiquantum wells (MQWs). This technique is based on measuring a change in surface reflectance due to the absorption nonlinearities induced by the carriers, and has a temporal resolution of ~1 ps. Typical results on a $GaAs/Al_xGa_{1-x}As$ MQW and an $In_{0.53}Ga_{0.47}As/In_{0.52}Al_{0.48}As$ MQW are compared. The observed fast transport times can only be explained by a field-dependent carrier emission out of the quantum well, after which transport through the continuum states can occur. Due to larger barriers in the $In_{0.53}Ga_{0.47}As/In_{0.52}Al_{0.48}As$ system, this intrinsic limit to transport is much larger, and hence these devices are observed to be slower than their $GaAs/Al_xGa_{1-x}As$ counterparts.

As material quality and processing techniques continue to improve over the years, the speed of optoelectronic devices using multiquantum wells (MQW) has improved to the point where intrinsic material characteristics, such as the carrier transport, recombination lifetime, etc., are expected to be important issues.[1] GaAs-based device structures have been the most investigated, owing to the maturity in the growth technology.[2] For 1.5-μm optical fiber communication applications, carrier dynamics and transport in InP-based material systems needs to be understood as well. Optical switching and computing at $\lambda = 1.5$ μm is an important area of research, with considerable interest in high speed electro-optic and electroabsorptive modulators. Most of these optoelectronic devices operate at high optical densities where, in order to prevent bleaching of the absorption, it is necessary to quickly remove the carriers out of the quantum wells[3] to their respective electrodes. The time it takes for this transport process to occur gives an intrinsic limit to the operating speed of the device. This perpendicular carrier transport in typical heterostructures with ~1 μm of active region occurs in the time scale of a few to several tens of picoseconds, depending on the particular structure. Time-of-flight measurement technique has been the most popular scheme for studying intrinsic transport properties of devices, where conventionally a carrier packet is injected either electronically[4] or by using a short pulse laser,[5] and the resulting current pulse at the other end of the device structure is detected electronically by a fast sampling oscilloscope. However, to achieve single picosecond time resolution, it is necessary to use all-optical techniques based on ultrashort pulse lasers for the injection as well as the detection of the carrier packet.

In this study we report on an all-optical time-of-flight measurement with single picosecond resolution, for studying transport in a variety of heterostructure and MQW devices in both GaAs and InP-based material systems. A short pulse femtosecond laser is used to photoinject a carrier population near one end of the vertical device structure as shown in Fig. 1. This carrier population will ultimately reach the other end, dictated by the transport properties of the device. The detection can be done optically, by monitoring the carrier induced change in the optical reflectance,[6] absorption, or photoluminescence[7] through a variable-time-delayed laser pulse. The presence of carriers causes absorption nonlinearities through bandfilling, bandgap renormalization, and free-carrier absorption. This in turn can be related to the changes in the reflectance (ΔR) through the Kramers–Kronig relations.[8] In our experiment we monitor the reflectance from both sides to determine the initial photoinjected and the final carrier distribution, as shown in Fig. 1.

The typical sample structure consists of a p-i(MQW)-n diode to study the electric-field dependence of the transport process. The samples are grown by solid source molecular-beam epitaxy (MBE) and the layer schematic is shown in Fig. 2, for the $GaAs/Al_xGa_{1-x}As$ ($x = 0.15$) and $In_{0.53}Ga_{0.47}As/In_{0.52}Al_{0.48}As$ devices. Mesa-etched diodes (diameter = 500 μm) were then fabricated, with annular p contacts on the top for optical access. To gain optical access from the backside, chemical etching is used to etch backholes in the GaAs and InP substrate, as depicted schematically in Fig. 2. Since optical reflectance is used to probe the carriers arriving at the surface, the etch-

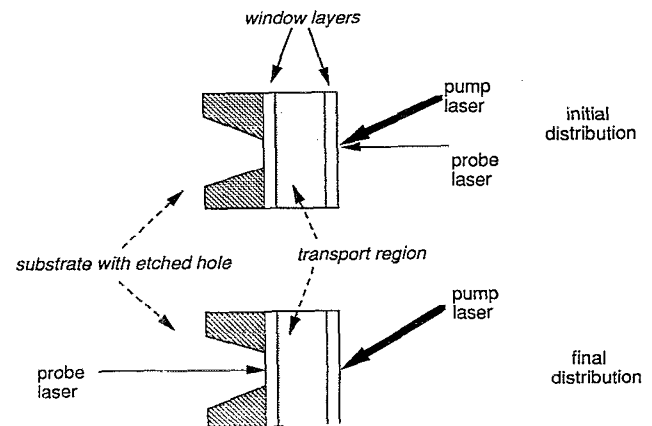

FIG. 1. Schematic of the all-optical time-of-flight measurement of transport in semiconductor heterostructures, using ultrashort laser pulses.

 © 1992 American Institute of Physics

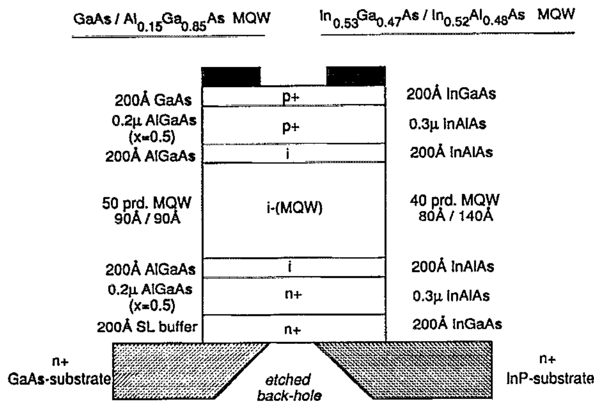

FIG. 2. Layer structure of the MBE grown $GaAs/Al_xGa_{1-x}As$ and lattice-matched $In_{0.53}Ga_{0.47}As/In_{0.52}Al_{0.48}As$ MQW.

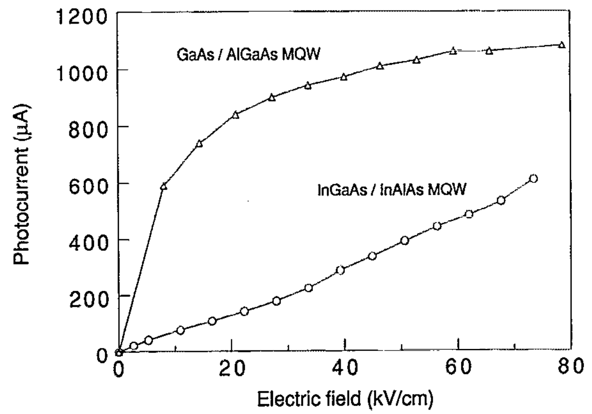

FIG. 3. Direct current photocurrent data vs electric field for a typical $GaAs/Al_{0.15}Ga_{0.85}As$ and $In_{0.53}Ga_{0.47}As/In_{0.52}Al_{0.48}As$ MQW.

ing technique should result in optically smooth surfaces. The details of the etching technique, which to the best of our knowledge, has been developed for the InP substrate for the first time, can be found in Ref. 9. Besides providing the $p+$ and $n+$ contacts, the window layers serve as mechanical support, as etch stop layers in the chemical-etching process, and also to confine the carriers at each end, which results in an increase in the detected signal ΔR. To generate carriers in the active region only and not in the window layers, a 100-fs visible colliding pulse mode-locked dye laser ($\lambda = 620$ nm) is used for the GaAs samples. For the InP-based devices a femtosecond Ti-sapphire laser tuned to a wavelength just below the $In_{0.52}Al_{0.48}As$ band edge is used. Since the laser noise spectrum shows typical $1/f$ noise with corner frequencies in several hundreds of KHz, high-frequency lock-in detection with frequency heterodyning[10] is used to detect small signal changes in $\Delta R/R$ down to 10^{-6}. This is especially important because low excitation densities have to be used to avoid significant space-charge screening of the applied field, as will be discussed later. All the measurements were done at room temperature.

It is important to know the transport times in p-i(MQW)-n diodes used for electroabsorption modulators and self-electro-optic effect devices (SEEDs), to optimize their high speed response. Figure 3 shows the dc photocurrent as a function of the true internal electric field for a 90-Å/90-Å $GaAs/Al_{0.15}Ga_{0.85}As$ MQW sample and a 80-Å/140-Å $In_{0.53}Ga_{0.47}As/In_{0.52}Al_{0.48}As$ sample. The laser wavelength is tuned to ~ 10 MeV above the $n=1$ absorption using a Ti-sapphire and color center lasers, for the GaAs/AlGaAs and InGaAs/InAlAs MQW, respectively. Very low excitation densities were used to avoid absorption bleaching effects. It is seen that the current "levels off" for the $GaAs/Al_xGa_{1-x}As$ sample, whereas even for high E fields it does not do so in the $In_{0.53}Ga_{0.47}As/In_{0.52}Al_{0.48}As$ sample. The total carrier escape rate from a quantum well[11] can be approximated as given below:

$$\frac{1}{\tau} \approx \frac{1}{\tau_r(E)} + \left[\frac{kT}{2\pi m_i L_w^2}\right]^{1/2} \exp - \left[\frac{H_i(E)}{kT}\right] + \frac{n\hbar\pi}{2L_w^2 m_i} \exp - \left[\frac{2L_b\sqrt{2m_{bi}H_i'(E)}}{\hbar}\right]. \quad (1)$$

The three terms represent recombination, thermionic emission, and tunneling, respectively, and are electric-field dependent, and are assumed to be independent in the above expression. This simple expression does not involve phonon-assisted scattering mechanisms,[11] which may become important for some structures as discussed later. The parameters $H_i(E)$ and $H_i'(E)$ represent effective barrier heights for the thermionic emission and tunneling process, respectively.[12] L_w is the well width, L_b the barrier width, the subscript "i" stands for electrons or holes, m_i is the effective mass in the well, and m_{bi} is the effective mass in the barrier. Recombination times in these MBE grown materials are ~ 1 ns, and due to the extremely thick barrier widths in the samples (90 and 140 Å) the tunneling rates are negligible, except at high fields. Hence carrier sweep-out is governed by the field-dependent thermionic emission over the barrier followed by transport to the respective electrode through the continuum states. For the $GaAs/Al_{0.15}Ga_{0.85}As$ sample, based on a finite square well model, we calculate the barrier heights seen by the $n=1$ electron and heavy hole subbands to be 82 and 67 MeV, respectively. For the $In_{0.53}Ga_{0.47}As/In_{0.52}Al_{0.48}As$ sample, similar calculation gives electron and hole barriers to be 375 and 273 MeV, respectively. Thus the *barriers for both types of carriers* are increased by a factor of more than 4 in the $In_{0.53}Ga_{0.47}As/In_{0.52}Al_{0.48}As$ sample. Hence from Eq. (1), the carrier escape through emission over the barrier and their subsequent collection is much more efficient in the $GaAs/Al_{0.15}Ga_{0.85}As$ sample than in the $In_{0.53}Ga_{0.47}As/In_{0.52}Al_{0.48}As$ sample, which would explain the observed photocurrent vs the electric-field dependence of Fig. 3 in the two samples.

The inset in Fig. 4 shows the all-optical picosecond time-of-flight measurement at $E \sim 50$ kV/cm for the above two samples. The initial photoinjected carrier distribution at the front surface (not shown in the figure for clarity)

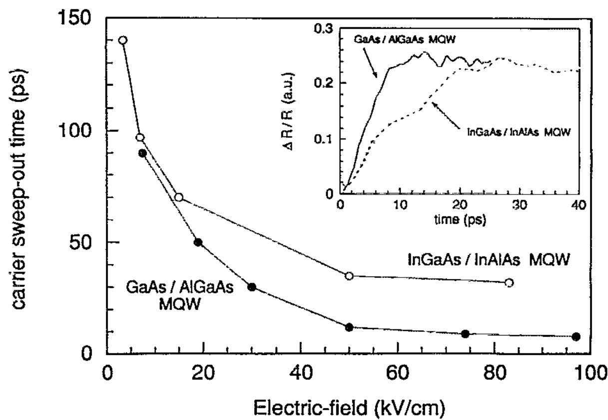

FIG. 4. Carrier transport times across the MQW region as a function of applied bias for a typical $GaAs/Al_{0.15}Ga_{0.85}As$ and $In_{0.53}Ga_{0.47}As/In_{0.52}Al_{0.48}As$ sample. (Inset) time-of-flight data for the above two samples at $E\sim50$ kV/cm.

shows a sharp "steplike" curve with $\sim$1-ps rise time, followed by a slow decay of several hundred picoseconds, determined by the trapping of carriers at the interfaces, and the transport away from this photoexcited region. Due to transport through the MQW region to the other end of the device structure, this leading edge will get smeared out in time. The rising edge of this final distribution, as detected at the opposite end of the device structure, gives a measure of the average transport time across the structure. This is observed to be $\sim$10 ps for the $GaAs/Al_{0.15}Ga_{0.85}As$ sample, whereas for the $In_{0.53}Ga_{0.47}As/In_{0.52}Al_{0.48}As$ sample this time is $\sim$32 ps. From Eq. (1), substituting the relevant parameters for the above two samples, at an applied bias corresponding to $E\sim50$ kV/cm, calculation shows that for the $GaAs/Al_{0.15}Ga_{0.85}As$ sample the thermionic emission over the barrier takes $\sim$1 ps, whereas the tunneling time is $\sim$28 ps. The drift time across the intrinsic region, assuming saturated drift velocity ($v=10^7$ cm/s) transport via the continuum states is <10 ps. Hence the transport is consistent with the picture of thermionic emission over the barrier followed by drift through the continuum states. For the $GaAs/Al_{0.15}Ga_{0.85}As$ system, similar very fast escape times have been measured in shallow ($x<0.06$) quantum wells.[13] For the $In_{0.53}Ga_{0.47}As/In_{0.52}Al_{0.48}As$ sample the thermionic emission time over the barrier is calculated to be orders of magnitude larger, due to the much higher barriers. However phonon-assisted scattering from lower subbands to higher confined states or the continuum can occur in several tens of picoseconds, followed by rapid tunneling or drift.[11] This could therefore explain the observed fast transport times in the $In_{0.53}Ga_{0.47}As/In_{0.52}Al_{0.48}As$ sample.

It should be noted that the photogenerated carriers, especially the holes, since they are trapped longer in the wells,[14] will lead to a space-charge screening of the applied electric field. For the low excitation density of $\sim$0.8 kW/cm^2 used in our experiment, this effect leads to about a 15% variation in the internal field over the intrinsic region, calculated on the same lines as in Ref. 14, and therefore does not qualitatively alter the results. From the time-of-flight measurements, we can also determine the carrier sweep-out time as a function of the applied bias for the above samples. This is depicted in Fig. 4. For low biases of $E<20$ kV/cm, the carrier sweep-out time is seen to increase rapidly. At higher fields this value saturates to $\sim$8 ps for the $GaAs/Al_{0.15}Ga_{0.85}As$ sample and to $\sim$30 ps for the $In_{0.53}Ga_{0.47}As/In_{0.52}Al_{0.48}As$ sample. Note that this is also a direct measure of the maximum operating speed of devices having a similar layer structure for the active region, under actual operating conditions. For room-temperature operation, the intrinsic limit to the response speed is primarily determined by the carrier escape out of the quantum well, and hence lower and thinner barriers are needed for faster response speeds. It should also be noted that due to the applied reverse bias and photoexcitation on the *p*-contact side, the electron transport is being measured.

In conclusion, we demonstrate the applicability of an all-optical time-of-flight technique using reflectance measurements, for directly measuring the intrinsic carrier transport in commonly used optoelectronic device structures with single picosecond time resolution. In particular, by comparing the transport in a $GaAs/Al_{0.15}Ga_{0.85}As$ and $In_{0.53}Ga_{0.47}As/In_{0.52}Al_{0.48}As$ sample, which have markedly different barriers, we show the importance of the field-induced carrier sweep-out from the quantum well in determining the intrinsic transport speed of an MQW structure.

The authors acknowledge Dr. Wei-qi Li for the MBE growth of the samples and Dr. J. Loehr and Professor J. Singh for discussions on the transport mechanisms. This work was supported by the Office of Naval Research under Grant No. N00014-90-J-1831 and the Army Research Office (URI program).

[1] A. M. Fox, D. A. B. Miller, G. Livescu, J. E. Cunningham, J. E. Henry, and W. Y. Jan, Appl. Phys. Lett. **57**, 2315 (1990).
[2] T. H. Wood, C. A. Burrus, D. A. B. Miller, D. S. Chemla, T. C. Damen, A. C. Gossard, and W. Wiegmann, Appl. Phys. Lett. **44**, 17 (1984).
[3] K. Wakita, I. Kotaka, O. Mitomi, H. Asai, Y. Kawamura, and M. Naganuma, J. Light. Technol. **8**, 1027 (1990).
[4] A. Neukermans and G. S. Kino, Phys. Rev. B **7**, 2693 (1973).
[5] R. A. Hopfel, J. Shah, D. Block, and A. C. Gossard, Appl. Phys. Lett. **48**, 148 (1986).
[6] B. F. Levine, W. T. Tsang, C. G. Bethea, and F. Capasso, Appl. Phys. Lett. **41**, 470 (1982).
[7] B. Deveaud, J. Shah, T. C. Damen, B. Lambert, A. Chomette, and A. Regreny, IEEE J. Quantum Electron. **QE-24** 1641 (1988).
[8] B. R. Bennett, R. A. Soref, and J. A. del Alamo, IEEE J. Quantum Electron. **QE-26**, 113 (1990).
[9] S. Gupta and P. K. Bhattacharya (unpublished).
[10] J. M. Chwalek and D. R. Dykaar, Rev. Sci. Instrum. **61**, 1273 (1990).
[11] A. Larsson, P. A. Andrekson, S. T. Eng, and A. Yariv, IEEE J. Quantum Electron. **QE-24**, 787 (1988).
[12] A. M. Fox, D. A. Miller, G. Livescu, J. E. Cunningham, and W. Y. Jan, Picosecond Electronics and Optoelectronics, Salt Lake City, Utah, 1991, paper WC3.
[13] J. Feldmann, K. W. Goosen, D. A. B. Miller, A. M. Fox, J. E. Cunningham, and W. Y. Jan, Appl. Phys. Lett. **59**, 66 (1991).
[14] T. H. Wood, J. Z. Pastalan, C. A. Burrus, B. C. Johnson, B. I. Miller, J. L. deMiguel, U. Koren, and M. G. Young, Appl. Phys. Lett. **57**, 1081 (1990).